Title

Evidence linking exposure of fish primary macrophages to antibiotics activates the NF-kB pathway.

Authors

Qiu, Wenhui
Hu, Jiaqi
Magnuson, Jason T
et al.

Publication Date

2020-05-01

DOI

10.1016/j.envint.2020.105624

Peer reviewed

Environmental Science & Technology

pubs.acs.org/est

Article

Transcriptomic Responses of Bisphenol S Predict Involvement of Immune Function in the Cardiotoxicity of Early Life-Stage Zebrafish (*Danio rerio*)

Wenhui Qiu, Bei Chen, Justin B. Greer, Jason T. Magnuson, Ying Xiong, Hanbing Zhong, Nicolette E. Andrzejczyk, Chunmiao Zheng,* and Daniel Schlenk*

Cite This: *Environ. Sci. Technol.* 2020, 54, 2869–2877

Read Online

ABSTRACT: Bisphenol S (BPS), an alternative for bisphenol A (BPA) that is present in thermal paper and numerous consumer products, has been linked to estrogenic, cytotoxic, genotoxic, neurotoxic, and immunotoxic responses. However, the mechanisms of BPS toxicity remain poorly understood. Here, following exposure to environmentally relevant concentrations ranging from 0.1 to 100 μg/L BPS, transcriptional changes evaluated by enriched gene ontology (GO), Kyoto Encyclopedia of Genes and Genomes (KEGG), and Ingenuity Pathway Analysis (IPA) predicted cardiac disease and impairment of immune function in zebrafish at the embryo-to-larvae stage. Consistent with impacts predicted by transcriptional changes, significant sublethal impacts were observed ranging from reduced heart rate [8.7 ± 2.4% reductions at 100 μg/L BPS treatment; $P < 0.05$] to abnormal cardiac morphology [atrial/ventricle area significantly increased; 36.2 ± 9.6% at 100 μg/L BPS treatment; $P < 0.05$]. RNA-sequencing analysis results also indicated changes in nitric oxide synthetase (NOS2) and interleukin 12 (IL12) after BPS treatment, which was confirmed at the protein level. Increased expression of other cytokine genes was observed in larvae, suggesting inflammatory responses may be contributing to cardiac impairment by BPS. BPS caused cardiotoxicity, which temporally corresponded with inflammatory responses as predicted from RNA sequencing and confirmed at the protein and cellular levels of biological organization. Additional study is needed to find causal linkages between these responses.

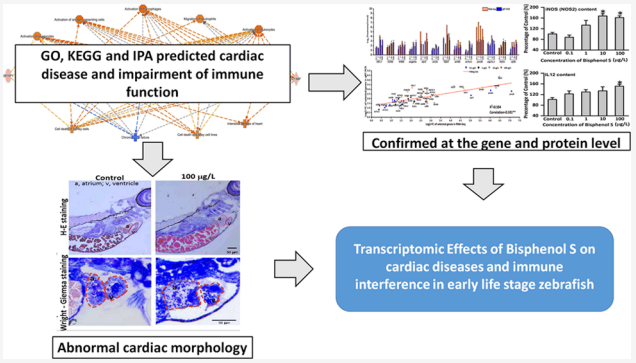

1. INTRODUCTION

Bisphenol S (BPS) is an emerging environmental contaminant commonly used as an alternative for bisphenol A (BPA) in the manufacturing of polycarbonate plastic, thermal paper, and numerous consumer products.[1,2] BPS has been detected in sediments (ND−1970 ng/g dw), sewage sludge (1.79−1480 ng/g dw), surface water (ND−7.2 ng/mL), and indoor dust (0.83−25 500 ng/g) in several countries.[3−6] BPS has further been detected in human serum (ND−0.1 ng/mL), urine (ND−29.261 ng/mL), maternal sera (ND−0.07 ng/mL), and cord sera (ND−0.12 ng/mL).[7,8] The concentrations measured within environmental samples and detected in aquatic and terrestrial organisms may pose significant risks to human health and the environment.[7,8] A systematic review of 22 previous in vitro and in vivo studies including human and aquatic organisms indicated that BPS exhibited estrogenic, cytotoxic, genotoxic, and neurotoxic effects similar to or even greater than those reported following BPA exposure.[9] Increased reproductive and neurotoxic effects as well as developmental malformations and behavioral effects in early life-stage fish following BPS have been reported.[9,10]

Low levels of BPS-induced neurogenesis in the hypothalamus of embryonic zebrafish and influenced hyperactive behavior in the resulting larvae.[11] In addition, embryonic zebrafish exposed to 0.5−25 mg/L BPS exhibited increased rates of estrogenic activity,[12] with oxidative stress and proinflammatory impacts further observed following BPS exposure in early life-stage zebrafish.[13−15] Perturbations to metabolism[16] and disruption in thyroid hormone concentrations,[17] glucose homeostasis,[18] and hematopoiesis[14] have also been noted. This suggests a broad-spectrum of BPS mechanisms and increased risk of BPS toxicity to biota. However, molecular initiating events preceding developmental and physiological defects are not well understood.

To better understand the multiple interacting molecular mechanisms that are altered during BPS exposure, global transcriptome sequencing (RNA-Seq) was performed in

Received: October 15, 2019
Revised: December 29, 2019
Accepted: December 31, 2019
Published: December 31, 2019

https://dx.doi.org/10.1021/acs.est.9b06213
Environ. Sci. Technol. 2020, 54, 2869−2877

embryonic fish to quantify expression levels of transcripts with a high sensitivity and broad genome coverage following BPS treatment.[19] To better understand the toxicity of environmentally relevant concentrations of BPS to fish, we evaluated morphological and transcriptional effects to determine the underlying mechanisms that regulate expression of transcripts altered by BPS. Downstream bioinformatic responses were compared between different exposure concentrations with subsequent morphological measurements to provide novel insights into the mechanisms of BPS-induced developmental toxicities in fish. This study provides potential phenotype-specific biomarkers through linking differentially expressed genes (DEGs) to toxicity endpoints, which could be useful in ecological risk assessments of BPS.

2. MATERIALS AND METHODS

2.1. Chemicals. BPS (CAS Number 80-09-1, 98%) was dissolved in dimethyl sulfoxide (DMSO) to obtain stock solutions of 10 g/L and stored at 4 °C. Test solutions (composition described below) of BPS were made in E3 medium (5 mM NaCl, 0.17 mM KCl, 0.33 mM $CaCl_2$, 0.3 mM $MgSO_4$). All chemicals used were of analytical grade and purchased from Sigma-Aldrich (St. Louis, MO).

2.2. Animals. Adult zebrafish (AB) were fed live brine shrimp (*Artemia nauplii*) twice daily in flow-through aquarium systems for a 14 h light/10 h dark photoperiod. Water temperature was maintained at 28 ± 0.5 °C. Embryonic zebrafish were collected within 1 hour post fertilization (hpf). Embryos were examined under a stereomicroscope, and unfertilized and poor-quality embryos were removed. All experiments were approved by the Institutional Animal Care and Use Committee at the Southern University of Science and Technology (SUSTC-JY2019067).

2.3. Experimental Design. Embryonic zebrafish (<4 hpf) were exposed to nominal BPS concentrations of 0.1, 1, 10, or 100 μg/L, or a solvent control (0.005% DMSO). These concentrations were based on the US Environmental Protection Agency guidelines for BPA allowed in drinking water (100 μg/L) to better understand the mode of action of BPA analogs in zebrafish development. A total of 100 embryos (<4 hpf) were randomly distributed into a glass Petri dish as one-sample pool and exposed to a dilute toxicant solution (200 mL) until 120 hpf, with each treatment run in triplicate. Exposure solutions were renewed daily. Larval zebrafish (120 hpf) were chosen for exposure as the embryo-to-larval stage is generally more sensitive to chemicals than adult stages.[20] Following BPS exposure, larvae were pooled per replicate, with each replicate flash-frozen in liquid nitrogen and stored at −80 °C for further RNA-Sequencing analysis. The concentrations of BPS in exposure solutions was measured after 24 h of treatment by liquid chromatography−mass spectrometry (LC−MS/MS; Agilent 1260 Infinity, Santa Clara, CA), as has been previously described.[15] Subsequent experiments were conducted following RNA-Seq to validate sequencing results.

2.4. RNA Isolation, cDNA Library Construction, and Sequencing. Larvae were collected and pooled (∼100 larvae) for RNA-Seq analysis, with each treatment run in triplicate. Total RNA was isolated and purified with TRNzol Total RNA Extraction Reagents (Tiangen Biotech Co., Ltd., Beijing, China) and RNA quality assessed by NanoDrop (Thermo Fisher Scientific, Waltham, MA) and Qubit (Invitrogen, Carlsbad, CA). An Agilent 2100 bioanalyzer chip was used to determine RNA integrity score (Agilent, Santa Clara, CA) with only high-quality RNA samples (28 S/18 S = 2.0−2.2, RIN > 9.0) used to construct libraries following a standardized procedure at the Beijing Genome Institute (BGI; Shenzhen, China). The libraries were sequenced at the Beijing Genomics Institute (BGI, Shenzhen, China) on a BGISEQ-500 platform with 50 bp pair-end reads, with three replicates per treatment group. All raw reads were deposited into the NCBI Sequence Read Archive (SRA accession: PRJNA595113).

2.5. Transcriptomic Analysis. Raw reads were analyzed by SOAPnuke (version 1.4.0) and trimmed using Trimmomatic (version 0.36). Specifically, the raw reads were filtered by SOAPnuke, under the following parameter: -l 5 -q 0.5 -n 0.1, to produce high-quality data via processes including the removal of adapter sequences, reads with ambiguous sequences (*N*) more than 5% and sequences with more than 20% low-quality bases (quality value < 10). The total number of raw reads and clean reads following quality control for each sample are listed in Table S1. The processed reads were mapped to the reference zebrafish genome using HISAT (version 2.1.0) and all reads were assembled using StringTie (version 1.0.4). Assembled reads were compared to the reference genome using Cuffcompare (version 0.9-r2) to predict new genes. The expression value of each gene was calculated using RSEM, with the per-gene and per-sample read counts provided as an independent file in Supporting Information. The differential expression of genes between control and treatment groups was determined using DEGSeq, with differential expression defined as fold-change ≥2 and adjusted *P*-value ≤ 0.001, as previously reported.[21] The total number of DEGs, both upregulated and downregulated, for each treatment is provided in Table S2. Phyper was used to perform gene ontology (GO) analysis (biological process, cellular component, and molecular function) and Kyoto Encyclopedia of Genes and Genomes (KEGG) pathways overrepresentation test, with a cutoff of false discovery rate (FDR) < 0.01 used. Ingenuity Pathway Analysis (IPA; Qiagen, Valencia, CA) was used to predict canonical pathways, disease and functions, and toxicity pathways (Table S3) based on differentially expressed genes between control and treatment groups.

2.6. Validation of Transcriptome Analysis using Quantitative Real-Time PCR (qPCR). Several DEGs identified in the IPA analysis were validated by qPCR. cDNA templates were generated using a Quant[17] Script RT Kit (Tiangen Biotech Co., Ltd., Beijing, China). Specific primers for the selected target genes were synthesized by Shenggong (China) (Table S4). *Rpl13a* (ribosomal protein L13a) was used as a reference gene, as previously conducted.[22] Melt curve analysis and 1% agarose gel electrophoresis were performed to assess the specificity of the qPCR products. Ct-based relative quantification with efficiency correction was normalized to *rpl13a*.[23] mRNA expression values were represented as mean (log2 fold-change) ± standard error of mean (SEM) (n = 3). Correlations between RNA-Seq and qRT-PCR results were analyzed by the linear-fitting method using OriginPro 8.0 and by Pearson correlation using SPSS Statistics 18.0 (SPSS Inc., Chicago, IL).

2.7. Nitric Oxide Synthase 2 (NOS2) and Interleukin 12 (IL12) Detection Assays. Considering NOS2 and IL12 were two of the highest-ranking responses determined by RNA-Seq analysis, the enzymatic activity of NOS2 and protein content of IL12 was measured following BPS treatment. The homogenate of larvae was centrifuged at 12 000×*g* for 20 min at 4 °C and the supernatant was eluted for analysis. NOS2

https://dx.doi.org/10.1021/acs.est.9b06213
Environ. Sci. Technol. 2020, 54, 2869−2877

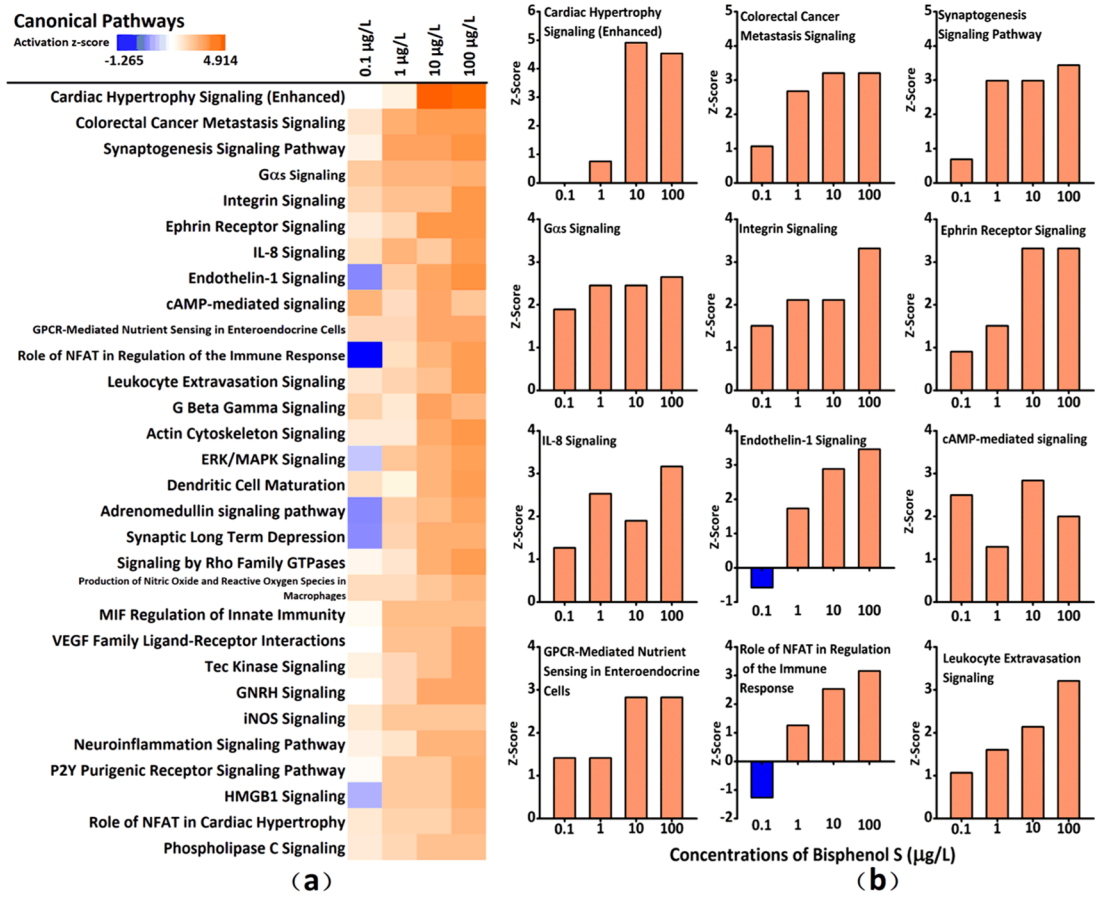

Figure 1. Canonical pathway analysis for 0.1, 1, 10, and 100 μg/L BPS exposure. Positive z-scores indicate predicted activation of a pathway, while negative z-scores indicate pathways predicted to be inhibited by BPS exposure. Z scores of ≥ 2 or ≤ -2 indicate that the upstream regulator was predicted to be activated or inhibited, respectively.

activity of the supernatant was measured colorimetrically at 530 nm, following the manufacturer's instructions (Nanjing Jiancheng Bioengineering Institute), based on NOS catalysis that converts amino acid L-arginine into citrulline with the generation of NO. The levels of IL12 in tissue homogenates were measured using a Fish Interleukin 12 ELISA Kit (Nanjing Jiancheng Bioengineering Institute) employing the quantitative sandwich enzyme immunoassay technique. An antibody specific for fish was precoated onto a 96-well microplate. A standard curve was constructed in parallel whenever the samples were tested. Each sample was run in triplicate. For ELISA analysis, the intraassay and interassay coefficients of variance (CV) were <10% and <12%.

2.8. Morphological Characteristics. Heart rate, defined as heartbeats per minute, was recorded at 120 hpf under a stereomicroscope. Heart rate was recorded from 12 larvae (n = 12) randomly selected from each exposure group.

To assess heart morphology, pathological slices were taken from 20 randomly selected larvae from each exposure group (n = 20), as previously described.[17] Briefly, zebrafish larvae were fixed in a 4% paraformaldehyde solution (pH = 7.2−7.4, Biosharp, China) overnight at 4 °C, washed in 1× phosphate-buffered saline (PBS, pH 7.4), and cryoprotected in 30% (w/v) sucrose (0.1 M PBS) at 4 °C overnight. Larvae were embedded in OCT, snap-frozen in liquid nitrogen, and stored at −80 °C. Larvae were sectioned at 8 μm thickness at −20 °C on a cryostat (Leica CM1900) and transferred to poly-L-lysine microscope adhesion slides. The tissue sections were stained by hematoxylin−eosin and Giemsa (Jiancheng, China), according to the manufacturer's instructions. Images were taken using a Leica Dmi8 microscope and analyzed using ImageJ. Hybridization of the lysozyme C gene was used to define the neutrophils present in cardiac sections. Whole-mount in situ hybridization was used to assess lysozyme C gene specificity in fish neutrophils following exposure to BPS at 120 hpf, with 16 larvae randomly selected from each exposure group (n = 16). The method for in vitro synthesis of probes and in situ hybridization was modified based on previous studies,[19] with further detailed information for in situ hybridization and neutrophil number calculated in the heart area provided in Supporting Information (text).

2.9. Statistics. Cluster analysis of DEGs was performed by the Hierarchical Clustering metric in "pheatmap" package of R.[21] A Fisher's exact test was used to determine the significance of the overlap between the regulator/diseases and disorder/Tox function and the responsive genes. Statistical analyses of NOS2 and IL12 levels and heart rate were analyzed by one-way analysis of variance (ANOVA) and Dunnett's test was performed to determine mean differences between control and exposure treatment groups (SPSS Statistics 18.0). Statistical analyses of atrium size (compared between control and the 100 μg/L BPS treatment only) were analyzed by Student's t-tests (SPSS Statistics 18.0). All data were considered normal based on the Kolmogorov−Smirnov one-sample test and Levene's test. The number of experimental units for each tested parameter is provided in Table S5.

https://dx.doi.org/10.1021/acs.est.9b06213
Environ. Sci. Technol. 2020, 54, 2869−2877

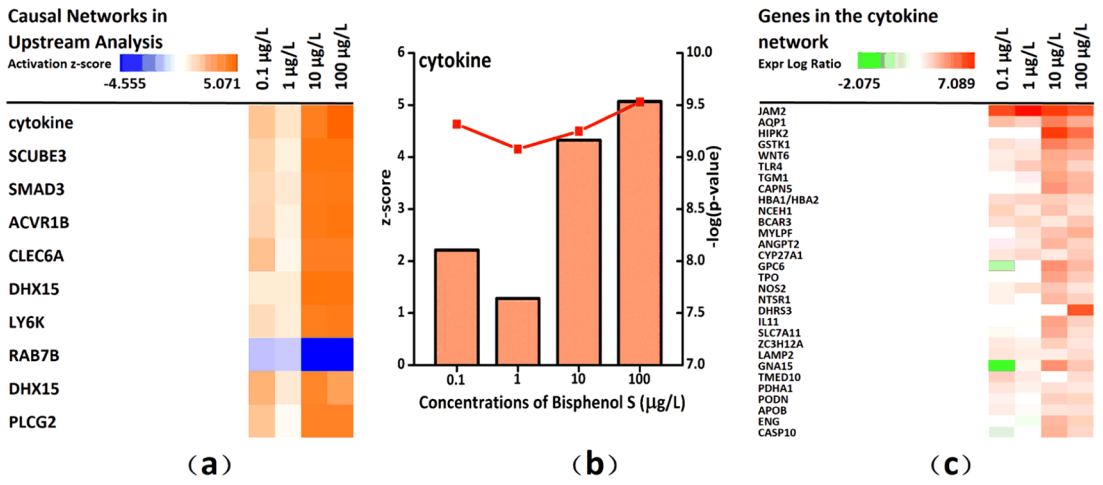

Figure 2. Cytokines present the most significantly activated genes in the causal network analysis. (a) Cytokine was the most relevant activated gene in the causal network analysis (Z scores ≥ 2, $-\log(P\text{-value}) > 1.3$). (b) The Z scores and $-\log(P\text{-value})$ of cytokine upon BPS treatments in causal network enrichment. The left Y-axis indicates the Z scores (orange column on the bottom) and the right Y-axis indicates $-\log(P\text{-value})$ determined by Fisher's exact test (red line on the top). (c) Top target genes of the cytokine network.

Significant differences versus control are indicated as $^*P < 0.05$.

3. RESULTS

3.1. Exposure Concentrations of BPS. No significant differences (less than 20%) between nominal and measured concentrations were detected (Table S6). Concentrations of BPS were undetectable in the control solution.

3.2. Transcriptome Analysis. To explore the molecular effects of BPS on fish growth and development, RNA-Seq was performed on zebrafish larvae following a 120 h exposure to BPS. A total of 1286.77 M BGISEQ-500 raw reads were generated. Following adaptor trimming and quality control, 1235.14 M clean reads were assembled with StringTie, with a Q20 percentage over 98% and Q30 percentage over 92%. For the remaining clean reads, the average percentage of reads mapping to the zebrafish (*Danio rerio*) genome for all groups was 87.20%. A total of 30 798 genes were detected in all samples, of which 26 211 genes were known and 4587 genes were not previously characterized. Each was quantified based on FPKM values (Fragments Per Kilobase per Million mapped fragments) by RSEM.

3.3. Identification of Differentially Expressed Genes (DEGs). A volcano plot (Figure S1) indicated significant DEGs obtained from RNA-Seq in each BPS exposure group with 594, 823, 2115, and 1573 genes significantly differentially expressed in the 0.1, 1, 10, and 100 μg/L treatments when compared to controls, respectively. Larvae exposed to 10 μg/L BPS had the most DEGs, with 1864 genes upregulated and 251 genes downregulated (Table S2). Among the four treatment groups, a cluster analysis of the DEGs expression profiles showed that most DEGs were altered in the same direction in all treatments (Figure S2). We further investigated the overlap of DEGs in the different BPS concentrations using a Venn diagram and found that a total of 113 genes were affected in all BPS exposure groups (Figure S3). The significant GO terms and KEGG pathways of each BPS exposure group were identified by the Phyper package (Figures S4 and S5). Analysis of GO terms showed BPS-induced changes in transcripts involved in cellular processes, biological regulation, and metabolic processes. For cellular processes, five of the top 15 genes were involved in cellular and organelle membranes. For molecular functions, two of the top 11 genes were involved in protein binding and catalytic activity (Figure S4, Q value ≤ 0.05). KEGG pathway analysis revealed signal transduction, cancer, immune system, infectious diseases, and the endocrine system as the top 6 ranked pathways (Figure S5, Q value ≤ 0.05). A similar enrichment of DEGs was found in GO terms and KEGG pathways analysis among BPS treatment groups, suggesting similar toxic effects, with regard to gene regulation, regardless of BPS concentration.

3.4. Canonical Pathways. IPA predicted significant activation of many of the same pathways across all BPS treatments, including cardiac hypertrophy signaling, colorectal cancer metastasis signaling, synaptogenesis signaling pathway, gas signaling, integrin signaling, ephrin receptor signaling, IL-8 signaling, endothelin-1 signaling, cAMP-mediated signaling, GPCR-mediated nutrient sensing in enteroendocrine cells, role of NFAT in regulation of the immune response, and leukocyte extravasation signaling ($-\log(P\text{-value}) \geq 1.3$; z-score ≥ 2) (Figure 1a). The top 30 predicted canonical pathways presented a concentration-dependent induction in response to increasing BPS exposure (Figure 1b). cAMP-mediated signaling (16 genes) was the highest ranked canonical pathway (z-score = 2.5, $-\log(P\text{-value}) = 2.92$) at 0.1 μg/L predicted by IPA and the synaptogenesis signaling pathway (19 genes) was the highest ranked at 1 μg/L (z-score = 2.982, $-\log(P\text{-value}) = 2.58$) (Table S7). Cardiac hypertrophy signaling (enhanced) (Figure S6) was the highest ranked canonical pathway at 10 and 100 μg/L (Table S7). Also, the IL-8 signaling pathway, the role of NFAT in the regulation of the immune response, and leukocyte extravasation signaling indicate that immune function or inflammation was impaired in zebrafish embryo-to-larvae stage.

3.5. Upstream Regulator Analysis and Diseases and Functional Analysis. The highest ranked activated and downregulated regulators in BPS-exposed zebrafish larvae are shown in Figure S7a. Most of the regulators predicted to be altered were affected in the same direction among 0.1, 1, 10, and 100 μg/L BPS exposures. Hepatocyte nuclear factor-1α (*hnf1a*) was predicted to be the top activated upstream regulator across all concentrations of BPS exposure. *Hnf1a* is a

https://dx.doi.org/10.1021/acs.est.9b06213
Environ. Sci. Technol. 2020, 54, 2869−2877

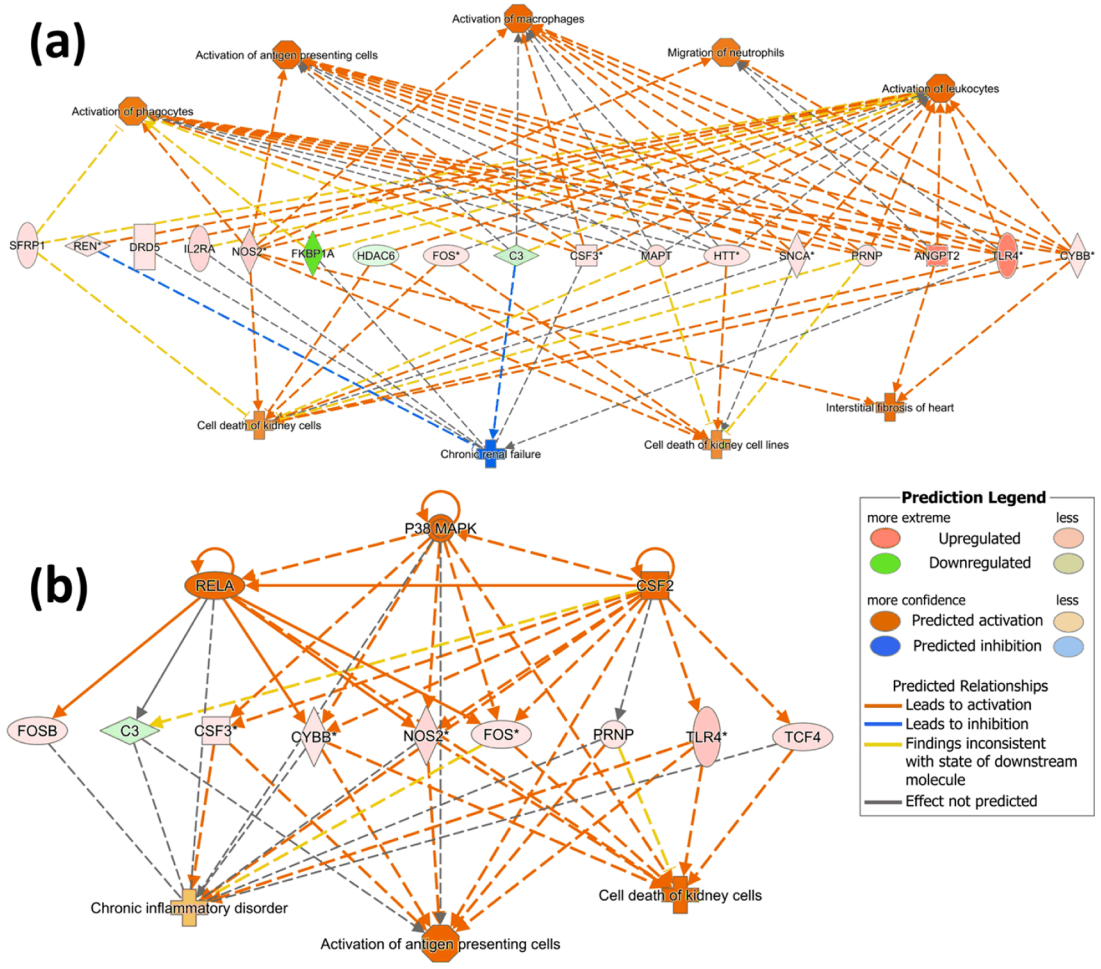

Figure 3. Predicted mechanisms through Ingenuity Pathway Analysis showing how bisphenol S (BPS) may lead to cardiac diseases, immune interference, and renal function impairment. Seventeen genes including *sfrp1*, *ren*, *drd5*, *il2ra*, *nos2*, *fkbp1a*, *hdac6*, *fos*, *c3*, *csf3*, *mapt*, *htt*, *snca*, *prnp*, *angpt2*, *tlr4*, and *cybb* (a) and three regulators including RELA, P38 MAPK, and CSF2 (b) are involved in both top diseases and disorders and toxicity predictions.

transcription factor and induces the expression of several liver-specific genes[24] including *cyp27a1*, *tmed10*, *zbtb20*, *apob*, *pax5*, *spo11*, *GCK*, *ttr*, *ugt2a3*, *gng12*, *pzp*, and *aldob*, all of which were upregulated in the present study. Another upstream regulator that was ranked second was colony-stimulating factor (*csf2*). *Csf2* (granulocyte−macrophages) is a cytokine that controls the production, differentiation, and function of granulocytes and macrophages. Many of its regulated genes are known to encode proteins involved in cytokine-mediated signaling pathways, cardiac hypertrophy signaling (enhanced), and innate and adaptive immune responses. Its target genes, *il12b*, *tlr4*, *nos2*, *trip13*, *lamp2*, and *fosl1*, were among the most highly upregulated genes in this study.

The top predicted diseases and disorders in zebrafish larvae following BPS exposure are shown in Figures S7b and S8. Activation of antigen-presenting cells ($P = 6.37 \times 10^{-5}$; Z score = 2.982 at 100 μg/L), migration of neutrophils ($P = 1.91 \times 10^{-4}$; Z score = 2.2 at 100 μg/L), activation of phagocytes ($P = 2.75 \times 10^{-5}$; Z score = 2.512 at 100 μg/L), activation of macrophages ($P = 1.21 \times 10^{-4}$; Z score = 2.758 at 100 μg/L), and activation of leukocytes ($P = 1.81 \times 10^{-7}$; Z score = 2.429 at 100 μg/L) were the top five enriched diseases and disorders in response to all BPS exposure concentrations. These enrichments are closely related to innate and adaptive immune diseases, inflammation, and cardiovascular system physiology.[25] Consistent with this, the highest ranked toxicity function prediction was interstitial fibrosis of heart (Figure S7c). The target genes of interstitial fibrosis of heart, including *angpt2*, *cybb*, *traf2ip2*, and *nos2*, were upregulated across all BPS exposure concentrations, with *angpt2*, *cybb*, and *nos2*, involved in the top five predicted diseases and disorders (Tables S8 and S9, Figure S9). Other highly ranked toxicity functions were cell death of kidney cell lines, cell death of kidney cells, end-stage renal disease, and chronic renal failure, suggesting toxic effects on kidney cells following BPS exposure (Figure S7c).

3.6. Causal Network Analysis (CNA). Causal network analysis (CNA) is a generalization of upstream regulator analysis that connects upstream regulators to data set molecules that takes advantage of paths that involve more than one link (i.e., through intermediate regulators), and can be used to generate a more complete picture of possible root causes for observed expression changes.[26,27] As shown in Figure 2a, cytokines were the most relevant activated regulator in the causal network analysis. One hundred and forty genes in our results were involved in cytokine networks with z scores of >4 and −log(P-value) > 9 among all treatment groups (Figure 2b). Seventy-eight percent of these genes were upregulated. Target genes of the cytokine network, *jam2*, *aqp1*, *hipk2*, *gstk1*, *wnt6*, *tlr4*, *tgm1*, *capn5*, *hba1/hba2*, and *nceh1*, were among the most upregulated genes in our data set (Figure 2c). The

https://dx.doi.org/10.1021/acs.est.9b06213
Environ. Sci. Technol. 2020, 54, 2869−2877

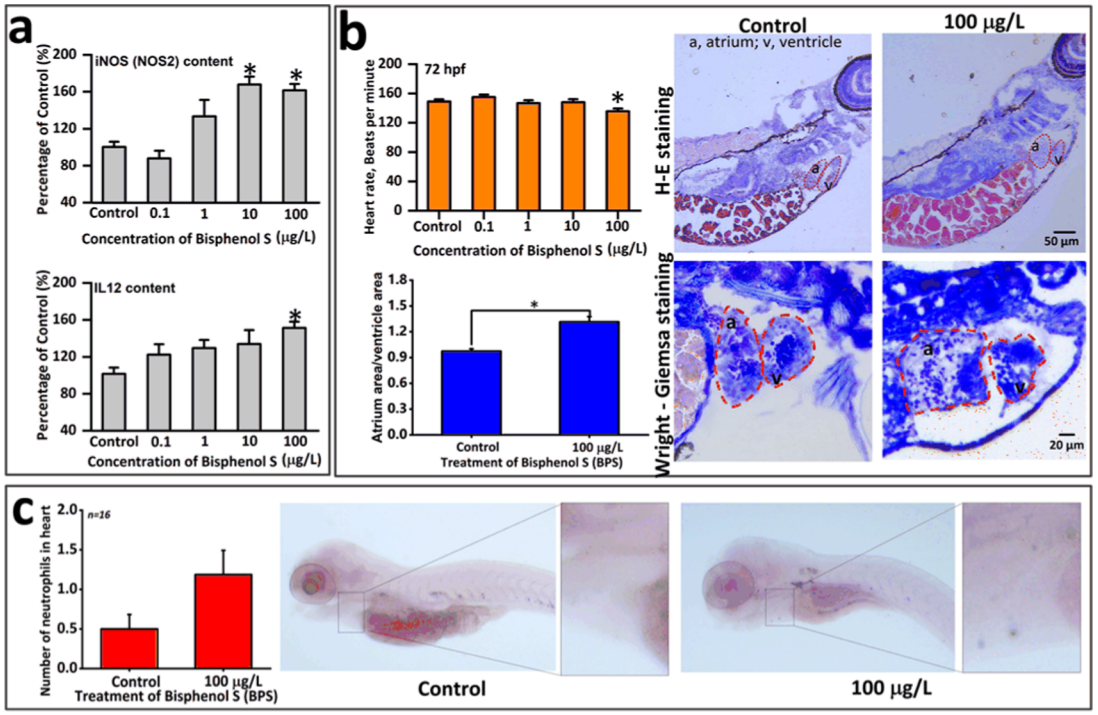

Figure 4. (a) Protein level of NOS2 and IL12 on BPS-treated zebrafish larvae. Values are means ± standard error of means (SEM) (n = 3). Significant differences versus the control are indicated as *P < 0.05 (ANOVA, Dunnett's). (b, c) Verification of IPA predicted cardiac diseases by heart rate (n = 12), pathological slices (n = 20), and in situ hybridization (n = 16). (b) Size of the atrium was found to largen after 100 μg/L BPS treatment as compared to control, determined from H−E and Wright−Giemsa staining (P < 0.05, T-test, n = 20). Control: atrium area = 0.00915 ± 0.0009 mm^2 (mean ± SEM). (c) The number of neutrophils within the fish heart was increased following BPS exposure, though not significantly (P > 0.05, T-test) (n = 16). a denotes atrium; v denotes ventricle.

observed alterations in gene expression following BPS exposure were predicted to result in a significant induction of cytokines in zebrafish larvae (Figure S10). The observed induction of cytokines could have detrimental effects during fish life cycles by affecting immune responses including apoptosis, leukopoiesis, and inflammatory responses (Figure S10).

3.7. Regulator Effects. The highest ranked diseases and disorders and toxicity predictions overlap several target genes (Figure 3a). Seventeen genes, including *sfrp1*, *ren*, *drd5*, *il2ra*, *nos2*, *fkbp1a*, *hdac6*, *fos*, *c3*, *csf3*, *mapt*, *htt*, *snca*, *prnp*, *angpt2*, *tlr4*, and *cybb* are involved in both top diseases and disorders and top toxicity predictions (Figure 3a). Overlapping genes of *fosb*, *c3*, *csf3*, *cybb*, *nos2*, *fos*, *prnp tlr4*, and immunoglobulin transcription factor *tcf 4* were involved in a regulator effects data set (Figure 3b). Three regulators of these genes were predicted to be induced by BPS exposure; RELA, P38 MAPK, and CSF2. The observed induction of regulators and their downstream genes could potentially evoke the activation of antigen-presenting cells, chronic inflammatory disorders, and cell death of kidney cells, which is consistent with predicted top diseases and disorders and top toxicity prediction analyses (Figure 3b).

3.8. Verification of Selected DEGs and Morphological Characteristics. The top DEGs identified in the pathway and function analysis by IPA were *il21r.2*, *il12bb*, *tlr4bb*, *angpt2a*, *vipr2*, *nos2a*, *hipk2*, *wnt6b*, *slc7a11*, *jam2b*, *aqp1a.2*, *hnf1a*, and *csf3b* genes, as shown in Table S10. The expression levels of these genes were also upregulated in our qRT-PCR analysis (Figure S11). Moreover, the correlation of fold-change of selected genes obtained by RNA-Seq and qRT-PCR were analyzed with R^2 = 0.594 and the Pearson correlation coefficients = 0.591 (**P < 0.001) (Figure S11). In addition, protein concentrations of NOS2 and IL12 also increased significantly (Dunnett's test, P < 0.05) in a concentration-dependent manner (Figure 4a). Functional and histological evaluations of cardiac function were consistent with cardiac hypertrophy signaling and interstitial fibrosis of heart predicted from RNA-Seq by IPA. As shown in Figure 4b, heart rate was significantly decreased (average 8.9% reduction) in the 100 μg/L BPS treatment compared to controls. No morphological changes in heart size or form were observed following BPS exposure. However, atrial size increased in larvae exposed to 100 μg/L BPS, as determined through H&E and Wright−Giemsa staining (Figure 4b). Furthermore, following exposure to 100 μg/L BPS, the atrial to ventricle area was significantly increased by 35.1%, relative to control (Figure 4b, blue column, n = 20). Hybridization of the lysozyme C gene was used to define the neutrophils present in cardiac sections. Though an increasing trend of neutrophils was seen in BPS-exposed larvae (average 137.5% induction at 100 μg/L), there were no significant differences when compared to controls (Figure 4c).

4. DISCUSSION

Due to increased use and associated health concerns, BPS has been well-studied over the past decade. However, most studies have focused on morphological and functional abnormalities, and the underlying molecular mechanisms that influence these downstream effects are less studied and not well understood.[28,29] Transcriptomic and bioinformatic approaches provide tools that can help predict pollutant toxicity and better understand the mechanism of action of a chemical.[30]

https://dx.doi.org/10.1021/acs.est.9b06213
Environ. Sci. Technol. 2020, 54, 2869−2877

The present study used a transcriptomics-based approach to assess the mechanisms of action of BPS in early life-stage zebrafish at environmentally relevant concentrations (0.1−100 μg/L).

Consistent with proarrhythmic effects of 10^{-9} M BPS on ex vivo rat hearts[31] and decreased hematological functions and induced cardiovascular effects following 30, 60, and 120 mg/kg BW/day in rats,[32] cardiac hypertrophy and interstitial fibrosis were the most highly enriched canonical and Tox function pathways in BPS-exposed zebrafish. Similar adverse effects on the cardiovascular response, heart function, and transgenerational cardiac malformations were observed following the exposure to BPA in fish,[33−35] possibly acting through an estrogenic mechanism.[36] Moreover, epidemiological studies in humans have reported correlations between increased urinary BPA concentrations and cardiovascular disease including coronary artery disease,[37] angina, and myocardial infarction,[38] and decreased heart rate.[39] However, the effects of BPS on cardiac and cardiovascular system function in teleosts have not been previously identified. This is the first study to link BPS exposure to adverse cardiac effects.

Immunoregulatory effects following BPA exposure has been well-studied, and recent studies have found comparable immune-disrupting effects following BPS exposure.[15] Embryonic zebrafish exposed to low levels of BPS have shown increased reactive oxygen species (ROS) content, nitric oxide synthase (NOS) activity, and expression of cytokines.[15] Increased inflammatory stress has been observed in in vivo studies chronically exposing juvenile common carp to BPS and in acute in vitro fish primary macrophages.[40,41] Zebrafish exposure to BPS has further been shown to modify the immune function in offspring with increased lysozyme activity and altered oxidative stress and inflammatory cytokines, resulting in decreased immune defenses in zebrafish.[13] We similarly found that immune system pathways were affected following BPS exposure in zebrafish embryos. Using IPA, immune system development and function were predicted to be the top-ranked targets in zebrafish larvae exposed to BPS with increased activation of antigen-presenting cells, phagocytes, macrophages, leukocytes, and migration of neutrophils (Figure S7). Similar results were seen in KEGG pathway analysis, with the immune system and infectious diseases as the top significantly enriched biological functions following BPS exposure.

In addition to cardiac diseases and impairment of immune function, renal function alterations were among the top predicted disease, and Tox function pathways affected following BPS exposure (Figure S7c). Similar renal effects were previously reported in mice exposed to a range of BPS concentrations (0.1−10 mM), with an influence on oxidative stress, cell viability, apoptosis, and >15% renal cell change.[42] However, pathways in IPA predicted renal failure, cell death of kidney cell lines (26 genes), cell death of kidney cells (31 genes), end-stage renal disease (10 genes), and chronic renal failure (15 genes) in zebrafish exposed to BPS, suggesting that future research is needed to further understand the toxicity of BPS to the renal system.

Upstream regulators were further evaluated using IPA in BPS-exposed zebrafish (Figure 2). Notably, cytokines remained the top-ranked activated upstream regulator in BPS treatments and occurred in a dose-dependent manner. Cytokines participate in many physiological processes including the regulation of inflammatory responses.[43] As shown in the present study, a number of cytokine genes are involved in cardiac diseases and inflammatory interference with overlapping pathways (Tables S8 and S9). Moreover, a significant induction of IL12 levels and a trend toward neutrophil increase in the heart area were accompanied with reduced heartbeats and increased atrial size (Figure 4). Together, BPS caused cardiotoxicity, which temporally corresponded with inflammatory responses as predicted from RNA sequencing and confirmed at the protein and cellular levels of biological organization. Additional study is needed to find causal linkages between these responses.

BPS exposure induced NO synthase (iNOS or NOS2), which was predicted to influence cardiac disease immune system function and renal function (Figure 3a). NOS2, which synthesizes nitric oxide (NO), can regulate many physiological and pathological processes including cardiovascular signaling,[44] innate immune system,[45] neural innervation,[46] renal hemodynamics, and excretory function.[47] Increased NOS2 transcript and protein expression following exposure to BPS and other bisphenols have previously been reported in in vivo and in vitro studies.[15,48] Enhanced NOS activity following skin wounds has been suggested to be important in site-specific movement of white blood cells and initiation of an inflammatory response.[49] Thus, our results further support the role of NOS2 in the potential mechanism underlying toxicity functions in larval zebrafish exposed to BPS and could be a phenotype-specific biomarker, linking DEGs to toxicity endpoints.

In addition to NOS2, Toll-like receptor 4 (TLR4) and cytochrome b-245 β chain (CYBB) were previously reported to be important genes involved in inducing inflammatory responses.[50] NF-κB, MAPK, CSF, JAK-STAT, and P13 K pathways were activated in human neutrophils through the stimulation of proinflammatory cytokines.[51] Three regulators, RELA, P38 MAPK, and CSF2 play an important role in regulating cytokines (*fosb*, *csf3*, *nos2*, *fos*, *prnp*, *tlr4* and *tcf 4*) and immune genes (*c3* and *cybb*) and were dysregulated by BPS. Moreover, significantly sustained upregulation subunits of STATs (STAT1, STAT3, STAT4, STAT5A, STAT5B, STAT5a/b), MAPKs (MAPK1, MAP3K1, MAP3K7, MAPK3, MAPK8, MAPK9, MAPK14, MAPKAPK2), and NFκB (NFKB1, NFKB1A, IKBKB, IKBKG) induce the upregulation of cytokines (Figure S10), and suggest a synergistic action of STATs, MAPKs, and NFκB in proinflammatory effects following BPS exposure. However, additional studies are needed to confirm these hypotheses.

In short, de novo transcriptomic assembly, gene expression, protein function, and immunohistochemistry were used to better understand the mechanisms of BPS toxicity during early life-stage zebrafish development. Comparisons of histological and biochemical responses with transcriptomic profiles were consistent with significantly differentially expressed genes, enriched gene ontology, functions and canonical pathways involved in cardiovascular and immune systems. These data indicate the upregulation of cytokines and NO may serve as upstream regulators involved in BPS pathogenesis, but further study is needed. The current study furthers our understanding of developmental effects in teleost and provides several biomarkers that are affected and could be used for assessing toxicity following BPS exposure.

https://dx.doi.org/10.1021/acs.est.9b06213
Environ. Sci. Technol. 2020, 54, 2869−2877

■ ASSOCIATED CONTENT

Supporting Information

The Supporting Information is available free of charge at https://pubs.acs.org/doi/10.1021/acs.est.9b06213.

In situ hybridization defined neutrophils; total raw reads and total clean reads; total DEGs; DEGs mapped in IPA; qPCR primers; experimental units number; BPS exposure concentrations; top canonical pathway and associated molecules; top predicted toxicity function genes; genes in the top disease and disorders; top two DEGs identified in top pathway and function; volcano plot; cluster analysis; Venn diagram of DEGs; significantly enriched GO terms and KEGG pathways; cardiac hypertrophy signaling pathway; upstream regulators; overlapping genes; comparison of mRNA levels of selected DEGs (Tables S1−S10 and Figures S1−S11) (PDF)

Number for per-gene and per-sample read counts, FPKM values (TXT)

■ AUTHOR INFORMATION

Corresponding Authors

Chunmiao Zheng − *Southern University of Science and Technology, Shenzhen, China;* orcid.org/0000-0001-5839-1305; Email: zhengcm@sustech.edu.cn

Daniel Schlenk − *University of California, Riverside, California*; Email: daniel.schlenk@ucr.edu

Other Authors

Wenhui Qiu − *Southern University of Science and Technology, Shenzhen, China, and University of California, Riverside, California;* orcid.org/0000-0002-9961-3928

Bei Chen − *Fisheries Research Institute of Fujian, Xiamen, China*

Justin B. Greer − *University of California, Riverside, California;* orcid.org/0000-0001-6660-9976

Jason T. Magnuson − *University of California, Riverside, California;* orcid.org/0000-0001-6841-8014

Ying Xiong − *Southern University of Science and Technology, Shenzhen, China*

Hanbing Zhong − *Southern University of Science and Technology, Shenzhen, China*

Nicolette E. Andrzejczyk − *University of California, Riverside, California;* orcid.org/0000-0003-4693-8654

Complete contact information is available at: https://pubs.acs.org/10.1021/acs.est.9b06213

Notes

The authors declare no competing financial interest.

■ ACKNOWLEDGMENTS

This work was sponsored by the National Natural Science Foundation of China (Grant 21707064), National Key R&D Program of China (2016YFC0402806 and 2018YFC0406504), State Environmental Protection Key Laboratory of Integrated Surface Water-Groundwater Pollution Control, Guangdong Provincial Key Laboratory of Soil and Groundwater Pollution Control (No. 2017B030301012), Shenzhen Science and Technology Innovation Committee (JCYJ20180302180205159 and KQTD2016022619584022), Southern University of Science and Technology (Grant No. G01296001), and the Leading Talents of Guangdong Province Program (Chunmiao Zheng).

■ REFERENCES

(1) Liao, C.; Liu, F.; Kannan, K. Bisphenol S, a new bisphenol analogue, in paper products and currency bills and its association with Bisphenol A residues. *Environ. Sci. Technol.* **2012**, *46*, 6515−6522.

(2) Le Fol, V.; Ait-Aissa, S.; Sonavane, M.; Porcher, J. M.; Balaguer, P.; Cravedi, J. P.; Zalko, D.; Brion, F. In vitro and in vivo estrogenic activity of BPA, BPF and BPS in zebrafish-specific assays. *Ecotoxicol. Environ. Saf.* **2017**, *142*, 150−156.

(3) Liao, C.; Liu, F.; Guo, Y.; Moon, H. B.; Nakata, H.; Wu, Q.; Kannan, K. Occurrence of eight bisphenol analogues in indoor dust from the United States and several Asian countries: implications for human exposure. *Environ. Sci. Technol.* **2012**, *46*, 9138−9145.

(4) Liao, C.; Liu, F.; Moon, H. B.; Yamashita, N.; Yun, S.; Kannan, K. Bisphenol analogues in sediments from industrialized areas in the United States, Japan, and Korea: spatial and temporal distributions. *Environ. Sci. Technol.* **2012**, *46*, 11558−11565.

(5) Yamazaki, E.; Yamashita, N.; Taniyasu, S.; Lam, J.; Lam, P. K. S.; Moon, H.-B.; Jeong, Y.; Kannan, P.; Achyuthan, H.; Munuswamy, N.; Kannan, K. Bisphenol A and other bisphenol analogues including BPS and BPF in surface water samples from Japan, China, Korea and India. *Ecotoxicol. Environ. Saf.* **2015**, *122*, 565−572.

(6) Yu, X.; Xue, J.; Yao, H.; Wu, Q.; Venkatesan, A. K.; Halden, R. U.; Kannan, K. Occurrence and estrogenic potency of eight bisphenol analogs in sewage sludge from the U.S. EPA targeted national sewage sludge survey. *J. Hazard. Mater.* **2015**, *299*, 733−739.

(7) Liu, J.; Li, J.; Wu, Y.; Zhao, Y.; Luo, F.; Li, S.; Yang, L.; Moez, E. K.; Dinu, I.; Martin, J. W. Bisphenol A metabolites and Bisphenol S in paired maternal and cord serum. *Environ. Sci. Technol.* **2017**, *51*, 2456−2463.

(8) Thayer, K. A.; Taylor, K. W.; Garantziotis, S.; Schurman, S. H.; Kissling, G. E.; Hunt, D.; Herbert, B.; Church, R.; Jankowich, R.; Churchwell, M. I.; et al. Bisphenol A, Bisphenol S, and 4-Hydroxyphenyl 4-Isoprooxyphenylsulfone (BPSIP) in urine and blood of cashiers. *Environ. Health Perspect.* **2016**, *124*, 437−444.

(9) Chen, D.; Kannan, K.; Tan, H.; Zheng, Z.; Feng, Y. L.; Wu, Y.; Widelka, M. Bisphenol analogues other than BPA: environmental occurrence, human exposure, and toxicity-A review. *Environ. Sci. Technol.* **2016**, *50*, 5438−5453.

(10) Igarashi, A.; Ohtsu, S.; Muroi, M.; Tanamoto, K. Effects of possible endocrine disrupting chemicals on bacterial component-induced activation of NF-kappa B. *Biol. Pharm. Bull.* **2006**, *29*, 2120−2122.

(11) Kinch, C. D.; Ibhazehiebo, K.; Jeong, J. H.; Habibi, H. R.; Kurrasch, D. M. Low-dose exposure to Bisphenol A and replacement Bisphenol S induces precocious hypothalamic neurogenesis in embryonic zebrafish. *Proc. Natl. Acad. Sci. U.S.A.* **2015**, *112*, 1475−1480.

(12) Lee, H.-J.; Woo, M.; Ok, S. Y.; Noh, J. S. Inhibitory effect of skate skin collagen on hepatic lipid accumulation through regulation of lipid metabolism. *J. Korean Soc. Food Sci. Nutr.* **2018**, *47*, 235−242.

(13) Dong, X.; Zhang, Z.; Meng, S.; Pan, C.; Yang, M.; Wu, X.; Yang, L.; Xu, H. Parental exposure to Bisphenol A and its analogs influences zebrafish offspring immunity. *Sci. Total Environ.* **2018**, *610−611*, 291−297.

(14) Lee, J.; Kho, Y.; Kim, P. G.; Ji, K. Exposure to Bisphenol S alters the expression of microRNA in male zebrafish. *Toxicol. Appl. Pharmacol.* **2018**, *338*, 191−196.

(15) Qiu, W.; Shao, H.; Lei, P.; Zheng, C.; Qiu, C.; Yang, M.; Zheng, Y. Immunotoxicity of Bisphenol S and F are similar to that of Bisphenol A during zebrafish early development. *Chemosphere* **2018**, *194*, 1−8.

(16) Qiu, W.; Liu, S.; Yang, F.; Dong, P.; Yang, M.; Wong, M.; Zheng, C. Metabolism disruption analysis of zebrafish larvae in response to BPA and BPA analogs based on RNA-Seq technique. *Ecotoxicol. Environ. Saf.* **2019**, *174*, 181−188.
(17) Lee, S.; Kim, C.; Shin, H.; Kho, Y.; Choi, K. Comparison of thyroid hormone disruption potentials by Bisphenols A, S, F, and Z in embryo-larval zebrafish. *Chemosphere* **2019**, *221*, 115−123.
(18) Zhao, F.; Jiang, G.; Wei, P.; Wang, H.; Ru, S. Bisphenol S exposure impairs glucose homeostasis in male zebrafish (*Danio rerio*). *Ecotoxicol. Environ. Saf.* **2018**, *147*, 794−802.
(19) Liu, F.; Wen, Z. L. Cloning and expression pattern of the lysozyme C gene in zebrafish. *Mech. Dev.* **2002**, *113*, 69−72.
(20) Mazurais, D.; Darias, M.; Zambonino-Infante, J. L.; Cahu, C. L. Transcriptomics for understanding marine fish larval development. *Can. J. Zool.* **2011**, *89*, 599−611.
(21) Wang, L.; Feng, Z.; Wang, X.; Wang, X.; Zhang, X. DEGseq: an R package for identifying differentially expressed genes from RNA-seq data. *Bioinformatics* **2010**, *26*, 136−138.
(22) Fan, C. Y.; Cowden, J.; Simmons, S. O.; Padilla, S.; Ramabhadran, R. Gene expression changes in developing zebrafish as potential markers for rapid developmental neurotoxicity screening. *Neurotoxicol. Teratol.* **2010**, *32*, 91−98.
(23) Pfaffl, M. W. A new mathematical model for relative quantification in real-time RT-PCR. *Nucleic Acids Res.* **2001**, *29*, No. e45.
(24) Shepherd, M.; Shields, B.; Ellard, S.; Rubio-Cabezas, O.; Hattersley, A. T. A genetic diagnosis of HNF1A diabetes alters treatment and improves glycaemic control in the majority of insulin-treated patients. *Diabetic Med.* **2009**, *26*, 437−441.
(25) Goerdt, S.; Orfanos, C. E. Other functions, other genes: alternative activation of antigen-presenting cells. *Immunity* **1999**, *10*, 137−142.
(26) Krämer, A.; Green, J.; Pollard, J., Jr.; Tugendreich, S. Causal analysis approaches in Ingenuity Pathway Analysis. *Bioinformatics* **2014**, *30*, 523−530.
(27) Xu, E. G.; Khursigara, A. J.; Magnuson, J.; Hazard, E. S.; Hardiman, G.; Esbaugh, A. J.; Roberts, A. P.; Schlenk, D. Larval red drum (*Sciaenops ocellatus*) sublethal exposure to weathered deepwater horizon crude oil: Developmental and transcriptomic consequences. *Environ. Sci. Technol.* **2017**, *51*, 10162−10172.
(28) Siracusa, J. S.; Yin, L.; Measel, E.; Liang, S.; Yu, X. Effects of Bisphenol A and its analogs on reproductive health: A mini review. *Reprod. Toxicol.* **2018**, *79*, 96−123.
(29) Qiu, W.; Zhan, H.; Hu, J.; Zhang, T.; Xu, H.; Wong, M.; Xu, B.; Zheng, C. The occurrence, potential toxicity, and toxicity mechanism of Bisphenol S, a substitute of Bisphenol A: A critical review of recent progress. *Ecotoxicol. Environ. Saf.* **2019**, *173*, 192−202.
(30) Mu, X. Y.; Huang, Y.; Li, X. X.; Lei, Y. L.; Teng, M. M.; Li, X. F.; Wang, C. J.; Li, Y. R. Developmental effects and estrogenicity of Bisphenol A alternatives in a zebrafish embryo model. *Environ. Sci. Technol.* **2018**, *52*, 3222−3231.
(31) Gao, X.; Ma, J.; Chen, Y.; Wang, H.-S. Rapid responses and mechanism of action for low-dose Bisphenol S on ex vivo rat hearts and isolated myocytes: evidence of female-specific proarrhythmic effects. *Environ. Health Perspect.* **2015**, *123*, 571−578.
(32) Pal, S.; Sarkar, K.; Nath, P. P.; Mondal, M.; Khatun, A.; Paul, G. Bisphenol S impairs blood functions and induces cardiovascular risks in rats. *Toxicol. Rep.* **2017**, *4*, 560−565.
(33) Lombó, M.; Fernandez-Diez, C.; Gonzalez-Rojo, S.; Navarro, C.; Robles, V.; Herraez, M. P. Transgenerational inheritance of heart disorders caused by paternal Bisphenol A exposure. *Environ. Pollut.* **2015**, *206*, 667−678.
(34) Cypher, A. D.; Ickes, J. R.; Bagatto, B. Bisphenol A alters the cardiovascular response to hypoxia in *Danio rerio* embryos. *Comp. Biochem. Physiol. C: Toxicol. Pharmacol.* **2015**, *174*−*175*, 39−45.
(35) Posnack, N. G.; Jaimes, R., 3rd; Asfour, H.; Swift, L. M.; Wengrowski, A. M.; Sarvazyan, N.; Kay, M. W. Bisphenol A exposure and cardiac electrical conduction in excised rat hearts. *Environ. Health Perspect.* **2014**, *122*, 384−90.
(36) Moreman, J.; Takesono, A.; Trznadel, M.; Winter, M. J.; Perry, A.; Wood, M. E.; Rogers, N. J.; Kudoh, T.; Tyler, C. R. Estrogenic mechanisms and cardiac responses following early life exposure to Bisphenol A (BPA) and its metabolite 4-Methyl-2,4-bis(p-hydroxyphenyl)pent-1-ene (MBP) in zebrafish. *Environ. Sci. Technol.* **2018**, *52*, 6656−6665.
(37) Melzer, D.; Osborne, N. J.; Henley, W. E.; Cipelli, R.; Young, A.; Money, C.; McCormack, P.; Luben, R.; Khaw, K. T.; Wareham, N. J.; Galloway, T. S. Urinary Bisphenol A concentration and risk of future coronary artery disease in apparently healthy men and women. *Circulation* **2012**, *125*, 1482−1490.
(38) Lang, I. A.; Galloway, T. S.; Scarlett, A.; Henley, W. E.; Depledge, M.; Wallace, R. B.; Melzer, D. Association of urinary Bisphenol A concentration with medical disorders and laboratory abnormalities in adults. *J. Am. Med. Assoc.* **2008**, *300*, 1303−1310.
(39) Bae, S.; Kim, J. H.; Lim, Y. H.; Park, H. Y.; Hong, Y. C. Associations of Bisphenol A exposure with heart rate variability and blood pressure. *Hypertension* **2012**, *60*, 786−793.
(40) Qiu, W.; Yang, M.; Liu, J.; Xu, H.; Luo, S.; Wong, M.; Zheng, C. Bisphenol S-induced chronic inflammatory stress in liver via peroxisome proliferator-activated receptor gamma using fish in vivo and in vitro models. *Environ. Pollut.* **2019**, *246*, 963−971.
(41) Qiu, W.; Yang, M.; Liu, S.; Lei, P.; Hu, L.; Chen, B.; Wu, M.; Wang, K. J. Toxic effects of Bisphenol S showing immunomodulation in fish macrophages. *Environ. Sci. Technol.* **2018**, *52*, 831−838.
(42) Zhang, R.; Liu, R.; Zong, W. Bisphenol S interacts with catalase and induces oxidative stress in mouse liver and renal cells. *J. Agric. Food Chem.* **2016**, *64*, 6630−6640.
(43) Van der Meide, P. H.; Schellekens, H. Cytokines and the immune response. *Biotherapy* **1996**, *8*, 243.
(44) Loscalzo, J.; Welch, G. Nitric oxide and its role in the cardiovascular system. *Prog. Cardiovasc. Dis.* **1995**, *38*, 87−104.
(45) Lowenstein, C. J.; Padalko, E. iNOS (NOS2) at a glance. *J. Cell Sci.* **2004**, *117*, 2865−2867.
(46) Bredt, D. S.; Hwang, P. M.; Snyder, S. H. Localization of nitric oxide synthase indicating a neural role for nitric oxide. *Nature* **1990**, *347*, 768−770.
(47) Bachmann, S.; Mundel, P. Nitric oxide in the kidney: synthesis, localization, and function. *Am. J. Kidney Dis.* **1994**, *24*, 112−129.
(48) Noguchi, S.; Nakatsuka, M.; Asagiri, K.; Habara, T.; Takata, M.; Konishi, H.; Kudo, T. Bisphenol A stimulates NO synthesis through a non-genomic estrogen receptor-mediated mechanism in mouse endothelial cells. *Toxicol. Lett.* **2002**, *135*, 95−101.
(49) Cals-Grierson, M. M.; Ormerod, A. D. Nitric oxide function in the skin. *Nitric Oxide* **2004**, *10*, 179−193.
(50) Levine, B.; Mizushima, N.; Virgin, H. W. Autophagy in immunity and inflammation. *Nature* **2011**, *469*, 323−335.
(51) Kato, T.; Kitagawa, S. Regulation of neutrophil functions by proinflammatory cytokines. *Int. J. Hematol.* **2006**, *84*, 205−209.

https://dx.doi.org/10.1021/acs.est.9b06213
Environ. Sci. Technol. 2020, 54, 2869−2877